AD-A033 651 AIR FORCE GEOPHYSICS LAB HANSCOM AFB MASS F/G 9/3
THE SAGAMORE HILL SWEEP FREQUENCY INTERFEROMETRIC RADIOMETER US--ETC(U)
AUG 76 D N GAUNT

UNCLASSIFIED AFGL-TR-76-0194 NL

1 OF 1
ADA033651

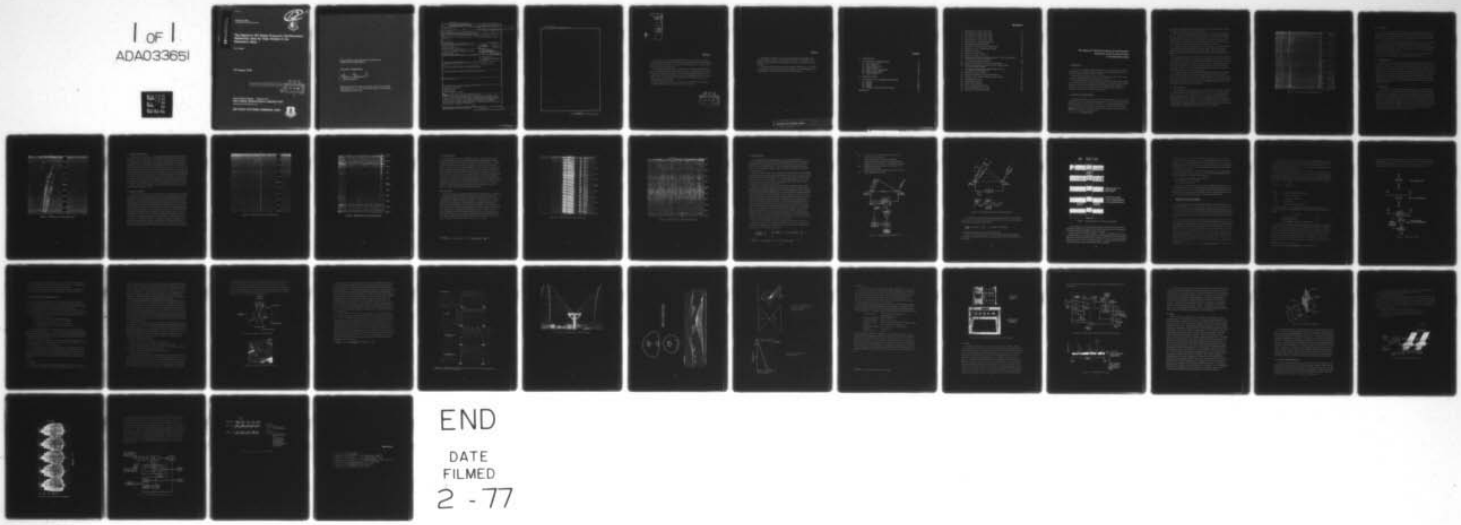

END

DATE
FILMED
2 -77

AFGL-TR-76-0194
INSTRUMENTATION PAPERS, NO. 248

The Sagamore Hill Sweep Frequency Interferometric Radiometer Used for Solar Studies in the Dekametric Band

D.N. GAUNT

23 August 1976

SPACE PHYSICS DIVISION PROJECT 4643
AIR FORCE GEOPHYSICS LABORATORY
HANSCOM AFB, MASSACHUSETTS 01731

AIR FORCE SYSTEMS COMMAND, USAF

This technical report has been reviewed and is approved for publication.

FOR THE COMMANDER:

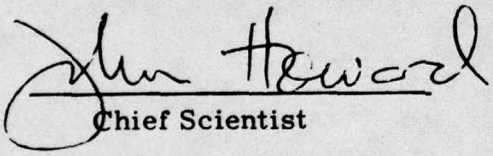

Chief Scientist

Qualified requestors may obtain additional copies from the Defense Documentation Center. All others should apply to the National Technical Information Service.

Unclassified

SECURITY CLASSIFICATION OF THIS PAGE (When Data Entered)

REPORT DOCUMENTATION PAGE

READ INSTRUCTIONS BEFORE COMPLETING FORM

1. REPORT NUMBER: AFGL-TR-76-0194
2. GOVT ACCESSION NO.
3. RECIPIENT'S CATALOG NUMBER
4. TITLE (and Subtitle): THE SAGAMORE HILL SWEEP FREQUENCY INTERFEROMETRIC RADIOMETER USED FOR SOLAR STUDIES IN THE DEKAMETRIC BAND
5. TYPE OF REPORT & PERIOD COVERED: Scientific. Interim.
6. PERFORMING ORG. REPORT NUMBER: IP No. 248
7. AUTHOR(s): D. N. Gaunt
8. CONTRACT OR GRANT NUMBER(s)
9. PERFORMING ORGANIZATION NAME AND ADDRESS: Air Force Geophysics Laboratories (PHP), Hanscom AFB, Massachusetts 01731
10. PROGRAM ELEMENT, PROJECT, TASK AREA & WORK UNIT NUMBERS: 62101F; 46430301; 03
11. CONTROLLING OFFICE NAME AND ADDRESS: Air Force Geophysics Laboratories (PHP), Hanscom AFB, Massachusetts 01731
12. REPORT DATE: 23 August 1976
13. NUMBER OF PAGES: 44
14. MONITORING AGENCY NAME & ADDRESS (if different from Controlling Office)
15. SECURITY CLASS. (of this report): Unclassified
15a. DECLASSIFICATION/DOWNGRADING SCHEDULE
16. DISTRIBUTION STATEMENT (of this Report): AFGL-TR-76-0194, AFGL-IP-248
Approved for public release; distribution unlimited.
17. DISTRIBUTION STATEMENT (of the abstract entered in Block 20, if different from Report)
18. SUPPLEMENTARY NOTES
19. KEY WORDS (Continue on reverse side if necessary and identify by block number)
Dekametric solar bursts
Type I-V events
Interferometer
Swept frequency radiometer
20. ABSTRACT (Continue on reverse side if necessary and identify by block number)

A sweep frequency interferometer covering the 25 to 75 MHz range at Sagamore Hill is described. The basic principles of sweep frequency interferometry are discussed. This report also describes the use and design of a Bicone antenna system, phase detector, and fringe width modulation technique—all developed at Sagamore Hill. The types of solar burst activity resolved with the system are reviewed.

DD FORM 1 JAN 73 1473 EDITION OF 1 NOV 65 IS OBSOLETE

Unclassified

SECURITY CLASSIFICATION OF THIS PAGE (When Data Entered)

409 578

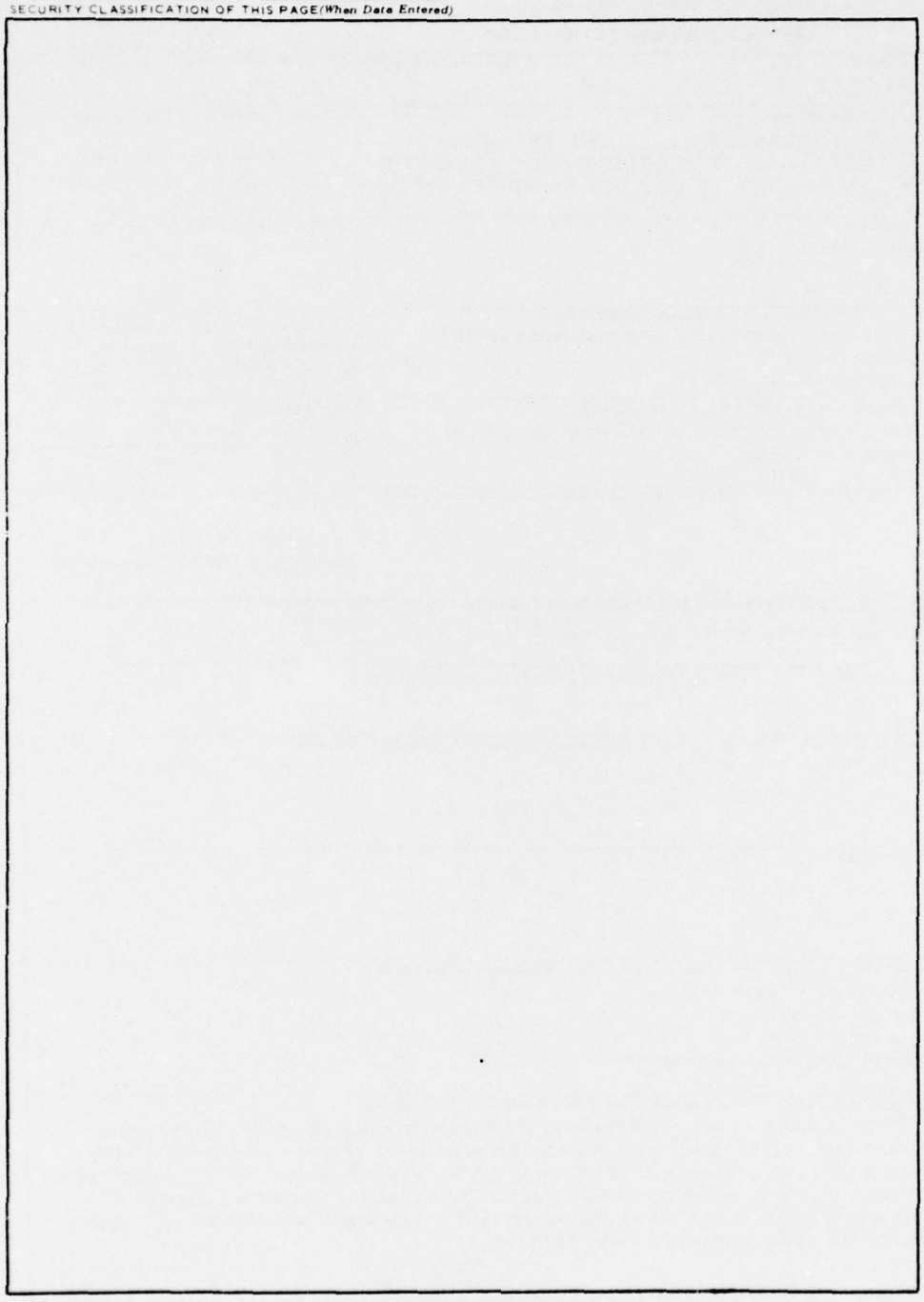

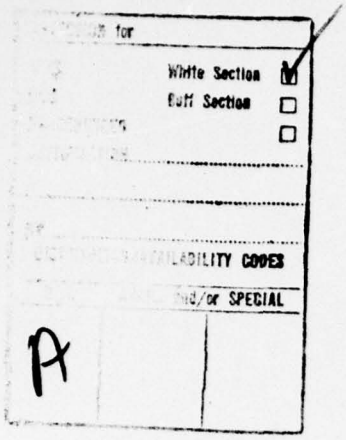

Summary

The design of the Sagamore Hill interferometer was the result of exclusive attention to the requirements of the special function it would serve, that of monitoring the Solar Radio spectrum in the meter and dekameter band on a continuous daily basis in a field site environment.

The experience of several years operation at the Sagamore Hill Observatory seems to confirm that these requirements were met. During this period, changes were made to enhance the value of the data, extending the bandwidth from 24 to 46 MHz to 25 to 75 MHz and adding a fringe width modulation circuit to increase the dynamic range of intensities over which individual, simultaneous events can be distinguished one from another.

Future addition to the system could include an automatic position resolving capability without requiring any basic changes in the system.

Preface

The author is indebted to John P. Castelli of AFGL for his guidance and assistance during the period of development of the SFIR. His perspective gave direction toward realizing the type and quality of data most valuable to the Solar Physicist.

The author also wishes to express his gratitude to Kenneth Eis, Capt, USAF, for his assistance in the preparation of this paper and in the understanding and consideration of operational needs of the Air Weather Service.

Contents

Illustrations

The Sagamore Hill Sweep Frequency Interferometric Radiometer Used for Solar Studies in the Dekametric Band

1. INTRODUCTION

Since 1965, the Sagamore Hill Radio Observatory has conducted an observational program for continuous daily measurement of the Solar Radio spectrum at nine fixed frequencies from 245 MHz to 35 GHz.

This has been in response to needs of continuing Solar research and, more recently, the operational requirements of the Air Force.

This report describes a sweep frequency interferometric radiometer, (SFIR) which has been added to the Sagamore Hill system to complement the nine discrete frequency systems. Also discussed are the considerations that shaped the development of the SFIR and the special features of data that are the subject of detection, measurement, and display of the system.

2. BACKGROUND AND OBSERVATIONS

Radio emissions from the sun were first detected by Hey in 1942. Systematic observations of these emissions was begun in 1946.[1] In the relatively short period of time since then, a very significant amount of the new information about the sun has come from these observations. As technology improved, the range of the spectrum observed by radio ground based systems has been extended to 100 GHz.

(Received for publication 20 August 1976)

1. Hey, J.S. (1946) Nature 157:47.

Atmospheric absorption of the higher radio frequencies makes observations above 100 GHz from ground stations extremely difficult.

Historically, optical observations have provided the earliest information about the sun. From white light and H-alpha observations one can observe photospheric and chromospheric details and deduce Solar magnetic field configurations via the Zeeman effect. The four octaves of information in the observed radio spectrum yield information about quiet and active sun magnetic fields, temperatures, electron densities, high energy particles, and other Solar parameters.

In addition to information about the sun, these observations yield data relevant to the Earth environment. Correlation has been observed between ionospheric phenomena and the 8,800 MHz Solar burst peak values. The centimeter burst spectrum has been used in forecasting polar cap absorptions and proton producing flares.

Presently the Air Force Air Weather Service (AWS) is tasked with the observation and prediction of Solar, and Solar induced ionospheric and particle phenomena. The Air Force system used for this purpose includes optical telescopes, magnetometers, satellite instruments, and Solar radio telescopes. The radio telescopes at Sagamore Hill observe at 9 discrete frequencies; 35 GHz, 15.4 GHz, 8.8 GHz, 4995 MHz, 2695 MHz, 1415 MHz, 606 MHz, 410 MHz, 245 MHz and a sweep frequency interferometer covering 25 to 75 MHz.

The Sweep Frequency Interferometric Radiometer (SFIR) which is the subject of this report, observes the Solar radio spectrum in the meter and dekameter band. The events observed have been classified according to their spectral character as they are observed on the records. This character is indicative of the mechanism which causes them, and in accordance with general agreement among Solar physicists are classified as described below.

2.1 Type I, Observations

Type I bursts (also called noise storms) are composed of two parts. The first is a series of bursts of short duration; 1/10 to 10 seconds. The series may continue for many days. Each burst when viewed individually has a frequency bandwidth of approximately 4 MHz and they occur most frequently between 100 and 200 MHz but do, at times, appear in the 20 to 100 MHz range. The second part is a long lasting, wide band continuum. This part usually extends over several tens of MHz and last minutes to hours and is very difficult to distinguish from the Type IV continuum. An example of a Type I burst is shown in Figure 1.

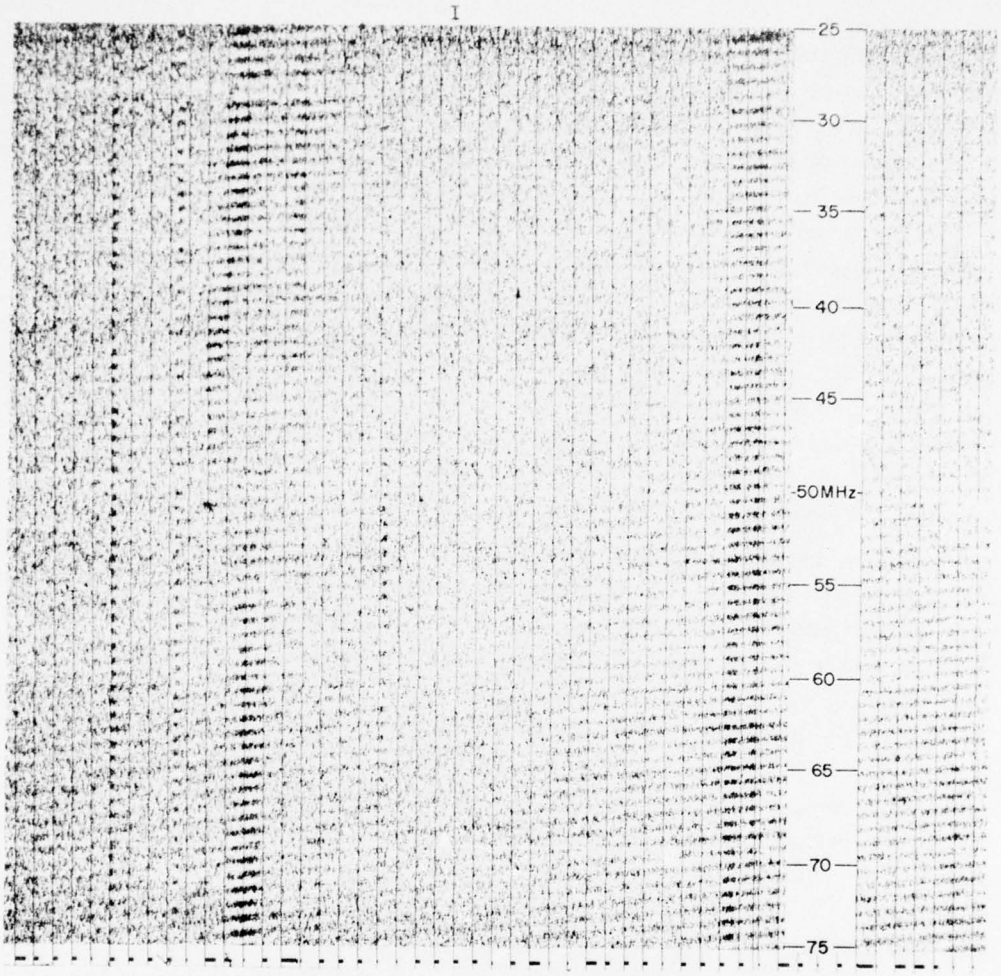

Figure 1. SFIR Record of a Type I Solar Event

2.2 Type I, Theory

Type I bursts are generally associated with sun spots and active regions. This association is not reciprocal in that all active regions are not Type I producers. Observations with high spacial resolution indicate that Type I radiation originates from small regions located high in the corona above sun spots. Two radio frequency generating mechanisms proposed for Type I are:

(a) Gyrosynchrotron radiation where electrons and other electrically charged particles ejected from the active region spiral in the coronal magnetic fields. While the charged particles are spiralling they emit radiowaves with an amplitude proportional to the magnetic field strength squared and frequency proportional to the velocity of the charged particles.

(b) Plasma radiation where fast particles from an active region excites the ionized ambient coronal plasma to oscillate at radio frequencies.

2.3 Type II, Observations

Observations of Type II bursts show a more complex character than those of the Type I noise storms, occurring less frequently than the noise storms. Type II bursts occur with a very high degree of correlation to large optical flares. Figure 2 shows the record of a Type II burst. The Type II drifts at rates between 0.25 and 1 MHz per sec starting at frequencies above 80 MHz and drifting to as low as 10 MHz. Type II's often show an abrupt low frequency cutoff. The time duration is generally 5 to 10 minutes. More than 60 percent of all Type II's show a harmonic structure, such as indicated in Figure 2. The harmonic is at about twice the fundamental frequency. Generally both the fundamental and harmonic show a split band structure.

2.4 Type II, Theory

The theories for Type II burst generation are numerous. All theories have one common aspect; an association with shock waves generated during the flash phase of a flare. This shock wave is sometimes identified by optical observations and appears as a brightening and darkening of photospheric and chromospheric structures. This disturbance moves out away from the flare site as an expanding circle. The velocity of the disturbance is of the order of 500 to 1500 km per second. The principal theory suggested to explain Type II's is the plasma hypothesis. This theory states that a disturbance generated at a low level in the sun's atmosphere ascends through the chromosphere and corona and excites the ambient plasma causing it to generate radio waves as it passes.

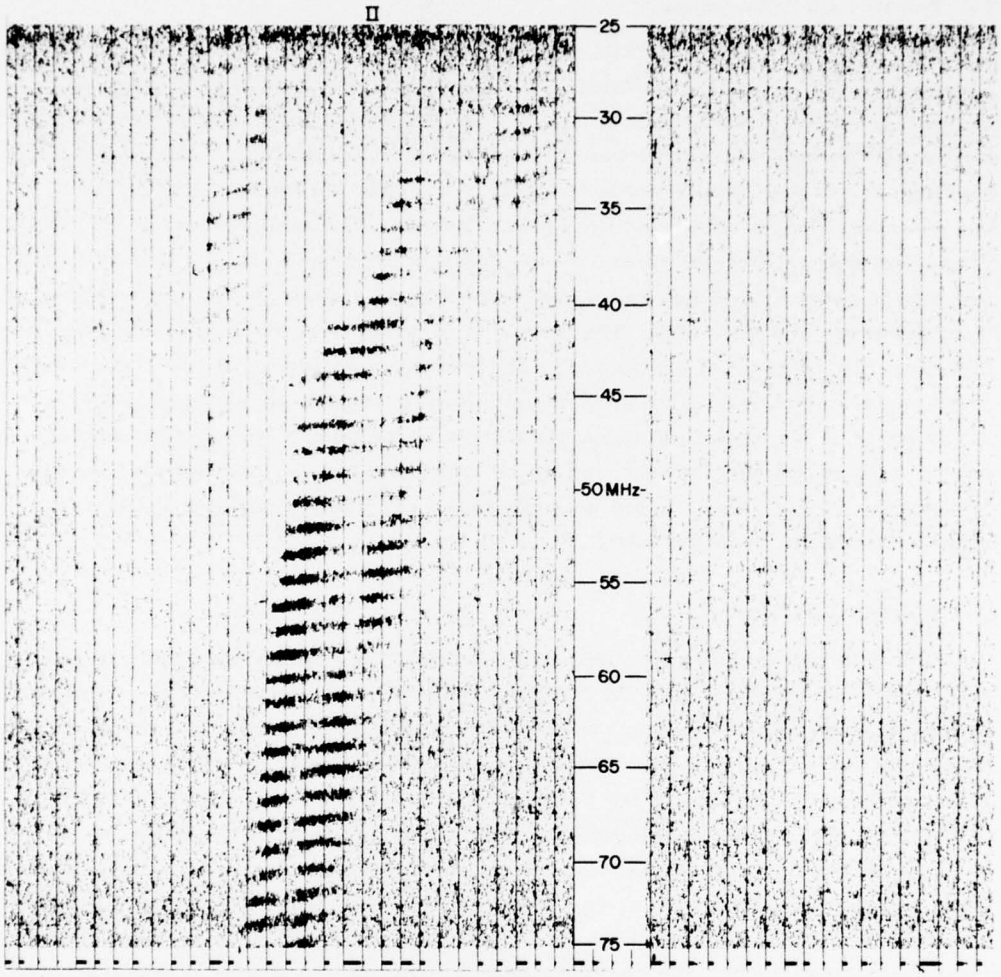

Figure 2. SFIR Record of a Type II Solar Event

2.5 Type III V and U Observations

The Type III, V and U bursts will be considered together in this section as they have many common characteristics. The Type III's have a drift rate from high to low frequencies of 1000 MHz to 1 MHz per sec, they show a harmonic structure in about 60 percent of occurrences in the range of 40 to 240 MHz. The leading and trailing edge of the Type III appears abruptly whereas the Type V trailing edge curves toward longer duration at the lower frequencies forming a sort of "V" image. These two types of bursts, III and V are shown in Figures 3 and 4. The Type III's duration is about 5 to 10 sec and never more than 30 sec for its full bandwidth which is in the order of 2 or 3 GHz. The Type V's duration is about the same as the Type III except the "afterglow" trailing edge at lower frequencies which can last 30 sec or so longer. The Type U burst is essentially the same in appearance as the Type III, however close inspection in the time scale at the higher frequencies reveals a split character merging as it moves to the lower frequencies forming an inverted "U" image. The split- or U-shape is the result of, first, a negative drift in frequency followed by a positive drift.

2.6 Type III V and U Theory

The drift rate of Type III bursts indicates that the stimulating agency is moving at a large fraction of the velocity of light. Since no phenomena has been observed optically on the sun, which approximates this speed, it is thought that the generating agency is charged particles having been electrostatically accelerated near the chromosphere and streaming out through the sun's atmosphere. First verification of this hypothesis came with interferometric observations confirming the velocity of the agency and the theory was assured when streams of electrons were observed in the vicinity of the Earth at a time related to the start time of the Type III burst. The outward moving electrons are guided by coronal magnetic fields. Some of these fields bend back to the sun's surface as suggested by optically observed coronal plasma into continuum emissions causing the trailing "afterglow" appearance of the Type V on the spectral records. The higher frequency continuum emission ends sooner than the lower frequency continuum because the damping effect is a function of the density of the region where emission is occurring, the higher density regions being near the surface of the sun where higher frequencies are emitted.

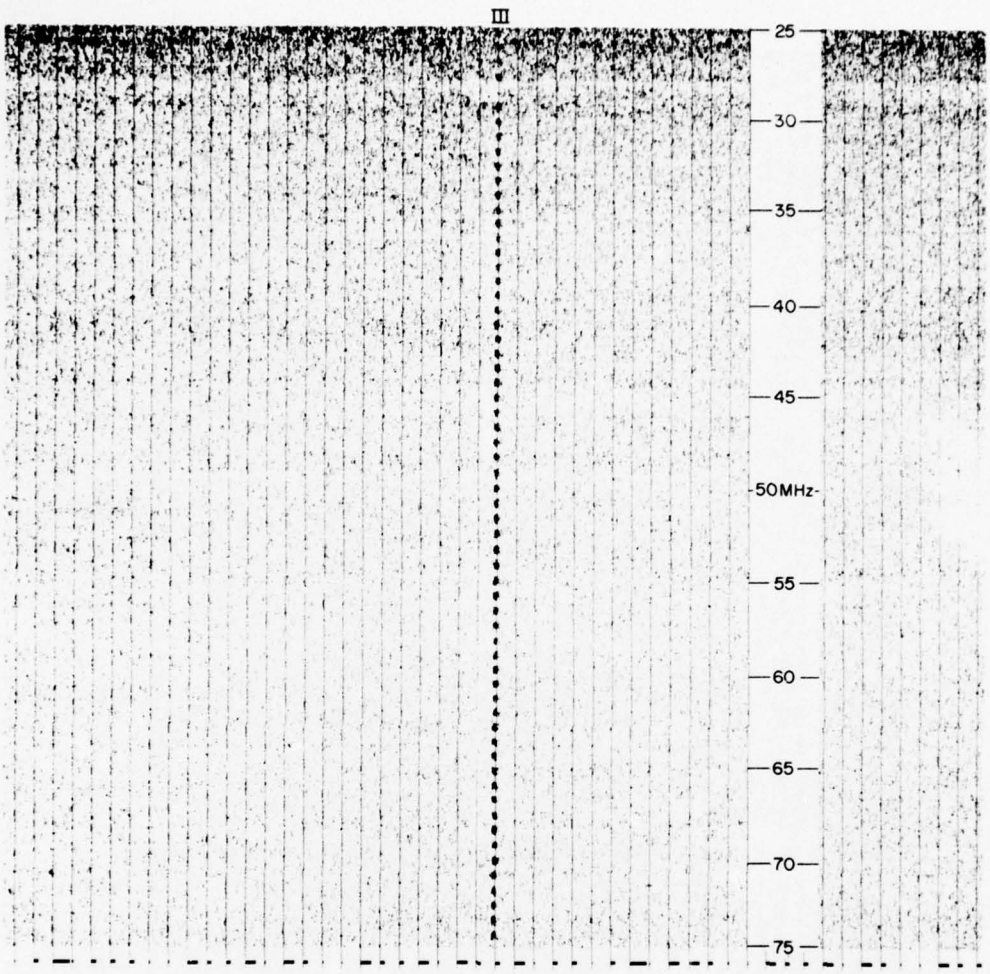

Figure 3. SFIR Record of a Type III Solar Event

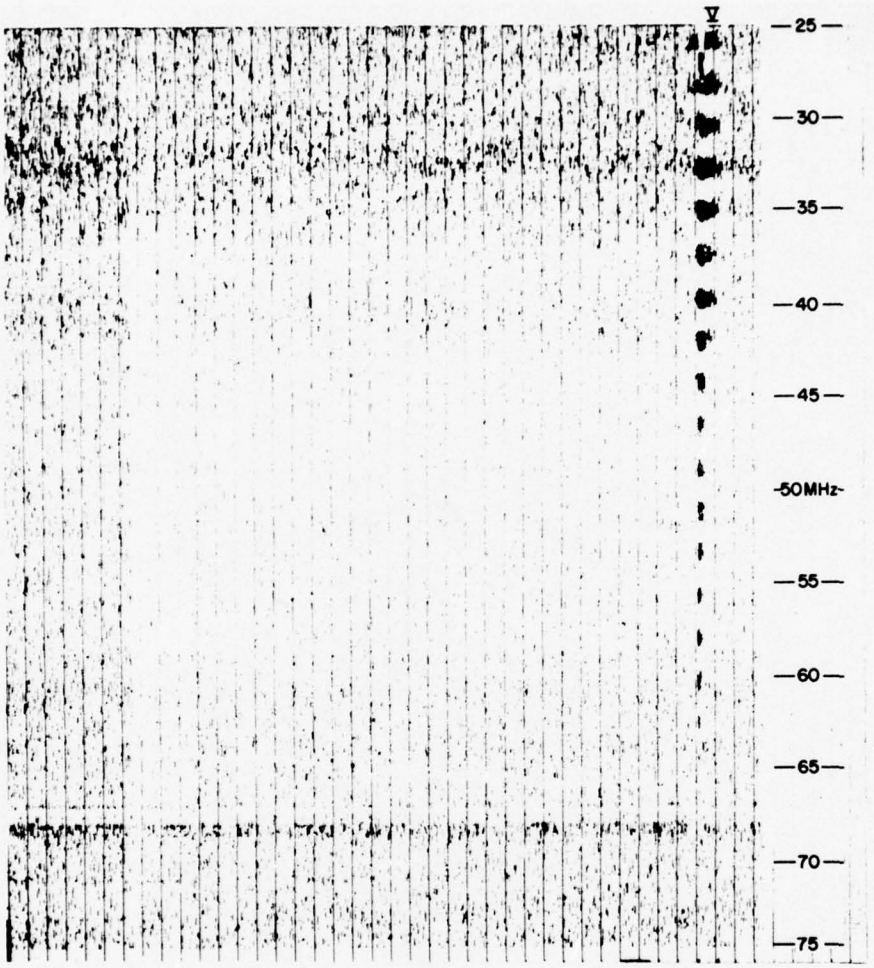

Figure 4. SFIR Record of a Type V Solar Event

2.7 Type IV Observations

Type IV bursts are difficult to categorize. This is due to the fact that the criteria identifying a Type IV have been different for each investigator. These criteria have resulted from historical evolution of the observations and the nature of equipment used. Because of this, the remarks on Type IV's will be general. Type IV's are observed as continuum radiation of a much smoother character than events classed as plainly continuum. Type IV's can show structure immediately after they begin but the bursty character of this structure will dampen out in a few tens of minutes. Type IV's have no continuous bursty component and generally last 30 min at cm wavelengths and 30 min to several hours at meter and dekameter wavelengths. Type IV's can be quite intense and often have a very gradual frequency drift to lower frequencies. This drift, unlike that of Type II's and III's, is very broadband and drifts at a rate on the order of 1 MHz per second. The source of Type IV radiation has been observed by interferometric systems to move, at times, in a range of velocities up to 1000 km per second.

2.8 Type IV Theory

Boischot and Denisse[2] proposed that the Type IV emission was due to relativistic electrons and protons spiraling in a magnetic field (synchrotron radiation). The intensity and broadband nature of the Type IV would have required a source at a temperature of 10^{12} K if bursts were to have a thermal origin, this is plainly ruled out. The synchrotron radiation mechanism described by Boischot and Denisse,[2] on the other hand, is more probably compatible with the physical conditions that exist. If one assumes electrons of 3 MeV kinetic energy (0.98c) moving in a magnetic field of 1 G to produce an observed flux of 1×10^{-19} W/cm^2/Hz, this would require 8×10^{32} electrons spiraling in the field. This number is the same order of magnitude as the number of protons associated with proton flares. This theory accounts for both the observed protons and electrons with one mechanism. Figures 5 and 6 show a classic Type IV and a continuum.

2. Boischot, A. and Denisse, K.V. (1957) Compt. Rend., 245:199.

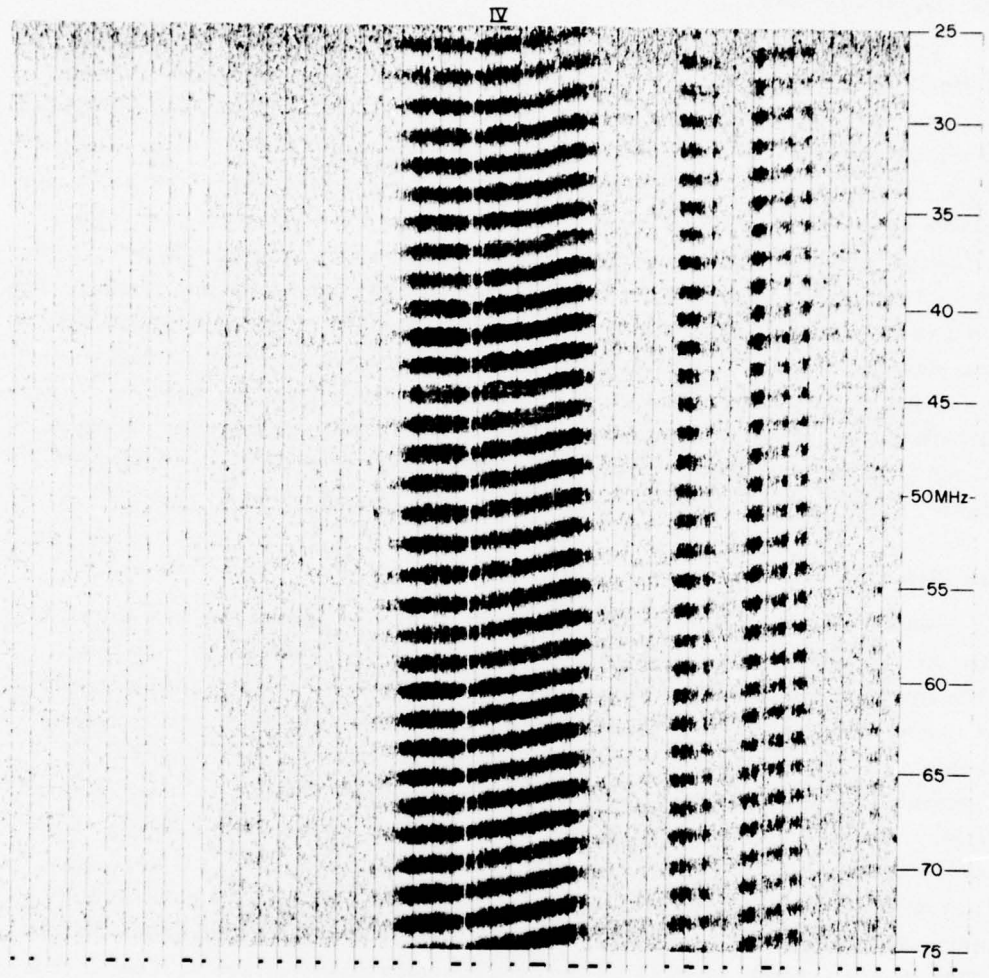

Figure 5. SFIR Record of a Type IV Solar Event

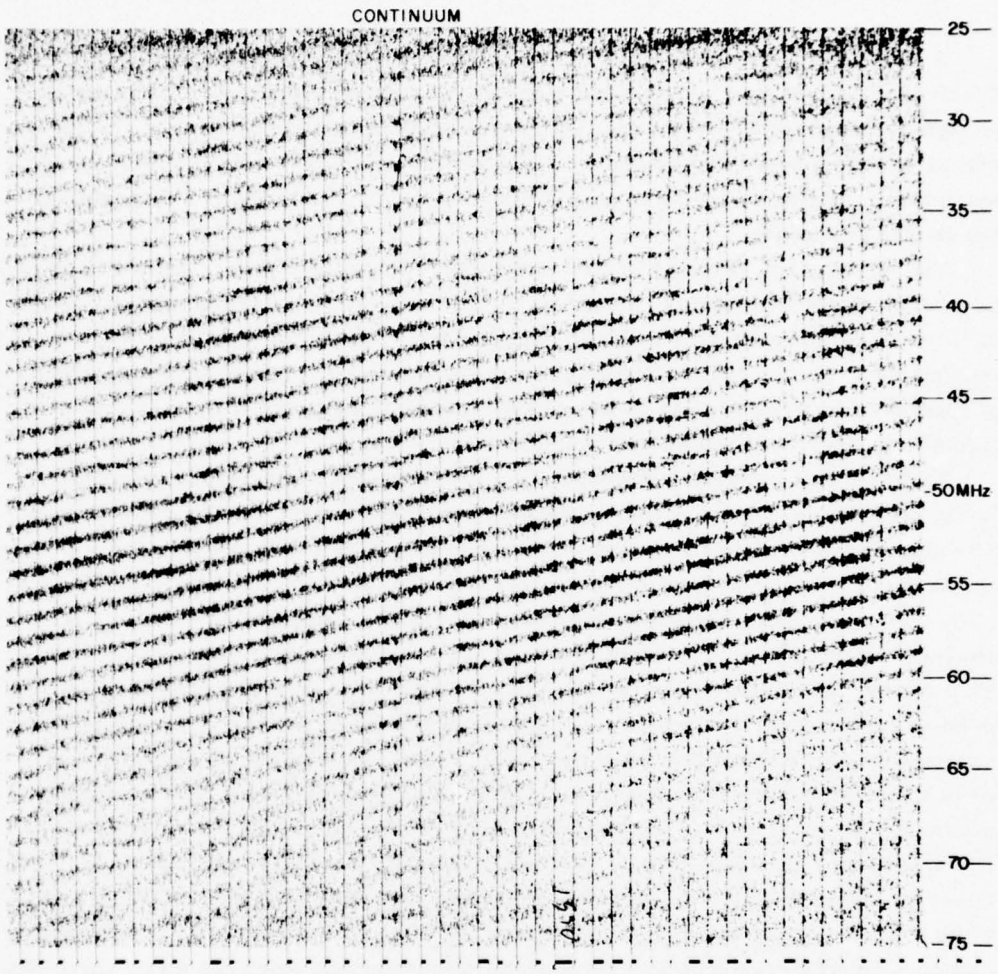

Figure 6. SFIR Record of a Continuum Solar Event

3. INSTRUMENTATION

A sweep frequency radio interferometer can generally be described as a specialized radiometric system that measures the phase difference and amplitude of signals from a discrete source, within a predetermined band, as they are received from two separated antennas. The measurements performed with such a system can provide information on position, amplitude, and spectral character of the source emissions.

There are many versions of this instrument in existence today; each is designed to emphasize some particular aspect of performance such as high sensitivity, source position resolution, or wide dynamic range. Their applications are also varied and fall in such areas as radio astronomy, surveillance, and spectral analysis. Most of these systems are similar in their basic design to the swept frequency interferometer described by Wild and Sheridan.[3]

Figure 7 is a functional diagram of a swept frequency interferometer; $x \sin \phi$ is the path difference of the signals received from the source via the two antennas. The distance separating the antennas is x, ϕ is the angle between a line to the source and the plane normal to the interferometer and d is the electrical length of the delay line. As the receiver sweeps in frequency, the path difference, $(x \sin \phi) + d$ will represent alternately, a multiple of one or a half wavelength of the received signal. This causes the phases of the two signals to alternately add and subtract at the point of comparison, the hybrid junction. If the receiver sweeps in frequency at a constant rate with respect to time the result at the receiver output will be a sine wave whose amplitude is proportional to the RF signal received from the discrete source. The separation of the peaks and nulls of this sine wave, in the frequency scale, will be a function of angle ϕ. This sine wave is usually recorded as an intensity variation on a time-frequency plot and appears as a series of black and white bands. The process which generates the sine wave is similar to that which produces interference fringes in an optical interferometer and in this text the peaks and nulls of this sine wave will be referred to as fringes.

When a source at position A, in a line at angle ϕ from a plane normal to the interferometer baseline, is displaced by an angle $\Delta\phi$ to position B, as shown in Figure 8, the relationship of the angular displacement of the source and the fringe displacement in the frequency dimension is

$$\left[\frac{F_m}{\frac{300}{(L \sin \phi) + d}}\right] \times \left[\frac{300}{(L \sin \phi) + d} - \frac{300}{[L \sin (\phi + \Delta\phi)] + d}\right] = f_d$$

3. Wild, J. P. and Sheridan, K. V. (1958) Proc. IRE, 46(No. 1):160.

where

F_m = frequency position of fringe whose displacement is to be measured (in MHz),

L = length of separation of antennas (in meters),

ϕ = angle between a plane normal to the interferometer baseline and a line to source at position A (in degrees),

$\Delta\phi$ = angular displacement of source from position A to position B (in degrees),

d = electrical length of transmission line delay, in meters,

f_d = fringe displacement (in MHz).

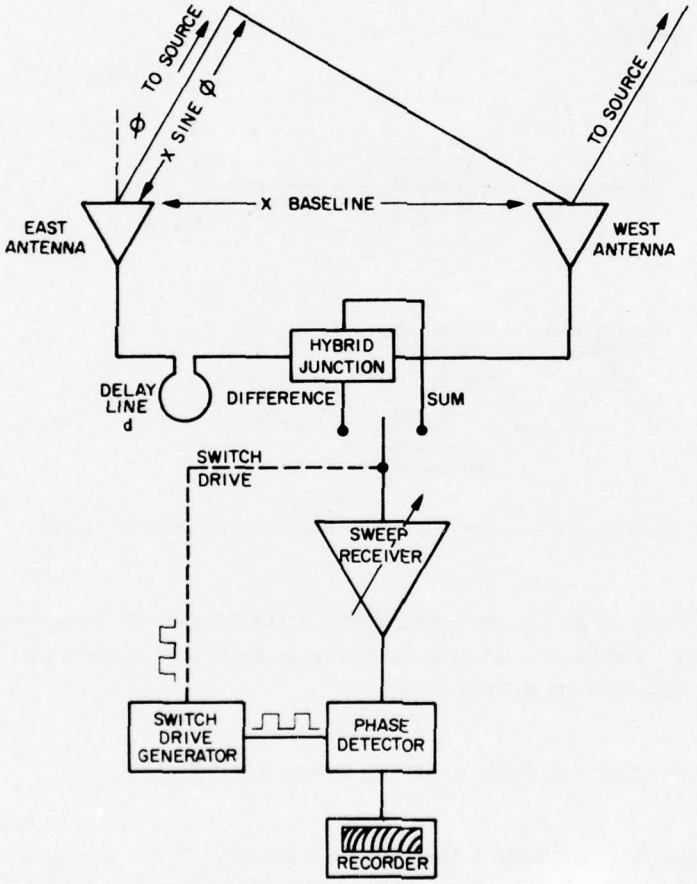

Figure 7. Multiplying Sweep Interferometer

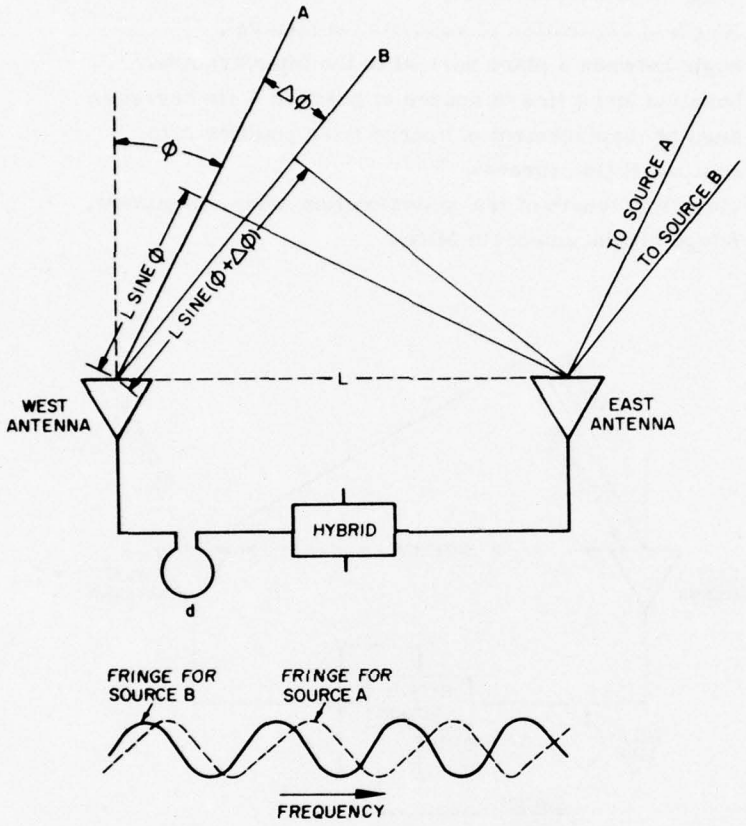

Figure 8. Relationship: Fringe to Source Displacement

As an example, in an interferometer with a baseline of 150 m and a transmission line of 75 m, a shift of 0.2° of a source from 5° to the vertical will cause the fringe at 57.9 MHz to shift 0.3429 MHz,

$$\frac{57.9}{3.6060} \times (3.4060 - 3.3754) = 17 \times 0.3060 = 0.3429 \text{ MHz},$$

(on the Sagamore Hill recorder 1 MHz = 0.26 inches).

Figure 9 is a sample record of a test made with the Sagamore Hill system showing the fringe shift resulting from the insertion of a 0.5 m delay addition to a 60 m delay.

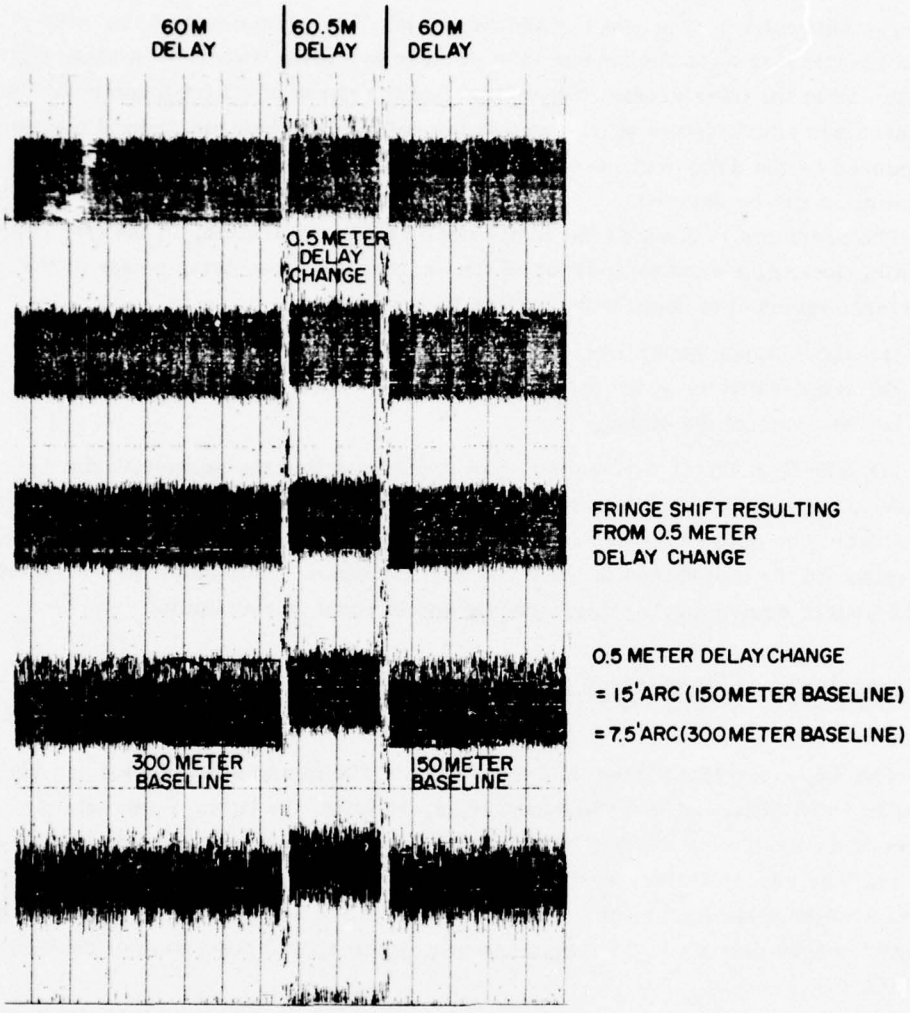

Figure 9. Fringe Shift From 0.5 Meter Delay Change

An interferometer can be described as being symmetrical or asymmetrical, depending on whether the lengths of transmission lines from each of the antennas to the point of phase comparison are equal or unequal.

When a delay line as shown in Figure 7, marked d, is inserted in one of the transmission lines, the interferometer becomes asymmetrical and the fringe separation in the frequency domain becomes a function of both (1) the free-space path difference x sin ϕ, and (2) the delay line length, d. Each has the effect of delaying the signal from source to the point of phase comparison.

The delay line is a necessary addition to produce asymmetry in the interferometer so that when the source is at or near meridian transit (in a plane perpendicular to the interferometer baseline) and the phase of all frequencies at the antennas are equal, phase differences at the point of comparison (hybrid junction) introduced by the delay will result in the generation of fringes from which phase information can be derived.

The precision with which the fringe position and separation, in the frequency domain, determine angular position of the source is the resolving power of the interferometer and is dependent on three factors:

(a) the distance separating the two antennas,

(b) the sensitivity of the system,

(c) strength of the signal.

(1) The first factor determines what could be called the geometric limit of resolution of the system. In a swept frequency symmetrical interferometric system it would be defined as the angular displacement of a source required to shift any fringe to the next fringe in the frequency domain or the angular displacement of the source equivalent to fringe spacing and is equal in radians to[4]

$$\frac{\text{Wavelength of the received signal}}{\text{Distance separating the antennas}} .$$

The Sagamore Hill system has a baseline of 300 m and sweeps once per sec from 25 to 75 MHz. At the mid-range point, 50 MHz, the limit of geometric resolution of the system or angular displacement equivalent to fringe spacing is 1.14°.

(2) The second factor, system sensitivity, is determined by antenna collecting area, system noise figure, and effective resolution of signal in noise (a composite of synchronous detection efficiency, integration time, and resolution of the output device).

In the Sagamore Hill system the sensitivity factor would be the accuracy with which the fringe position and separation could be determined in the frequency scale. For a signal of 50 flux units, this is approximately 1 part in 10 by visual determination and perhaps 1 part in 100 by electronic, digital or analog process. The sensitivity factor times the geometric resolution will equal the net system resolution which for visual processing would be about 15 min of arc and for electronic processing would be about 1.5 min of arc. Resolution of the fringe position could be improved by integration of the measurement of several fringe positions; however, there is a trade off in resolution. The source has frequency and physical dimensions, a gain in the resolution in one dimension can be realized by a proportionate reduction in the other.

4. Steinberg, J.L. and Lequeux, J. (1963) Radio Astronomy, McGraw Hill, p. 26.

It may be stated generally that an interferometer (unfilled aperture) can have the resolving power of a solid reflector telescope (filled aperture) whose diameter would be equal to the separation of the two antennas of the interferometer. It is obvious, however, that the difference in collecting area of the two systems means a proportional difference in sensitivity.

The method of comparing two antenna signals is a function of receiver design and the detection process. Depending on its configuration the interferometer can be defined as a simple interferometer or a phase switched, multiplying interferometer. These configurations are shown in Figure 10 and are compared with a total power receiver. The minimum detectable signal (temperature) of these systems is:

$$\Delta T_{min} = K_s \frac{NT_s}{\Delta F_{if} \times t_{pd}},$$

where

ΔT_{min} = minimum detectable temperature,

K_s = sensitivity constant,

NT_s = system noise temperature,

ΔF_{if} = IF bandwidth,

t_{pd} = post detection integration time.

The one variable which distinguishes these radiometer systems is K_s, the sensitivity constant. The relationship of K_s with respect to these systems is as follows[5]

System type	K_s*
Total power receiver	1
Simple interferometer	1/2
Phase switched multiplying interferometer	2

Theoretically, switching of the input and capturing the information by synchronous detection results in decreased sensitivity because the receiver is coupled, at any one time, to only one-half the power available from the antennas. Switching, essentially, measures the difference between two inputs by alternately connecting these to the receiver and synchronously detecting the resultant difference at the output. This confines the desired information to a narrow band centered on the switching frequency, and permits (by filtering) the enhancement of information relative to noise. One of the most significant components of noise is due to receiver

*Larger number means less sensitivity.

5. Kraus, J. D. (1966) Radio Astronomy, McGraw Hill, p. 258.

gain fluctuations which often can be 50 or 100 times greater than the minimum detectable signal. It can be seen that the overall sensitivity of a switched system with synchronous detection, though theoretically less, can, in practice, be much greater than in a non-switched system such as a simple interferometer.

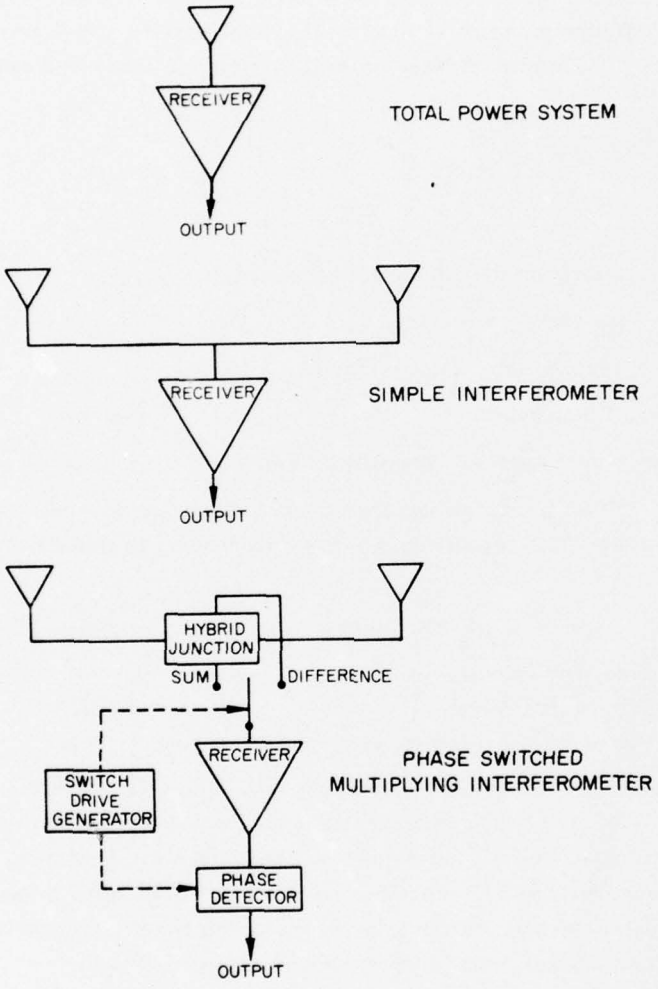

Figure 10. Radiometer Systems

(3) The third factor which determines system resolution is signal strength. It is obvious that given a certain sensitivity factor for a system, the stronger the signal the more precisely can the fringe position be defined.

The Sagamore Hill system, described here, is a multiplying interferometer and has a minimum detectable signal of approximately 10×10^{-22} W/m^2/Hz.

4. EVOLUTION OF THE SAGAMORE HILL SYSTEM

The present Sagamore Hill system is a phase sensitive, swept frequency radiometer used as an interferometer in a standardized configuration specifically for continuous measurement of the Solar Radio spectra in the meter and dekameter band. This application dictates the following design considerations.

(1) It should be modular in construction and design, using standard components, yet adaptable in a particular configuration to achieve the specialized function of monitoring Solar Radio emissions with the following general requirements:

(a) Sweep; 25 to 75 MHz,

(b) Dynamic range; 60 dB (logarithmic response),

(c) Minimum detectable signal; 10×10^{-22} W/m^2/Hz,

(d) Basic hardware which will allow later addition of a circuit for automatic source position resolution better than 15 min of arc.

(2) Selection of the modular components should make maximum use of pre-engineered off-the-shelf items. This requirement arises from logistics considerations as well as initial production costs. It is particularly important as the system must be adaptable for location at remote sites where maintenance and operational support can be relatively expensive.

(3) The application is one of long term (years) continuous measurements so reliability, stability, and repeatability of calibrations are very important in maintaining continuity of measurement standards.

The requirements and guidelines for the design of this system have evolved over a period of several years in the successive operation of three interferometer systems at Sagamore Hill Observatory in South Hamilton, Massachusetts. The present system may best be described by treating separately its main functional divisions, which are: (1) Antenna, (2) Receiver, (3) Detector, and (4) Output and Display.

4.1 Antenna

In the process of selection of a broadband antenna in the meter and dekameter band, one will most probably first consider a log periodic antenna. This type of

antenna, in general, will have nominal gain (6 dB) and reasonable linear response over the range of 1 or 2 octaves. However, the SWR of a log periodic for a range of this size can be of the order of 2:1 or greater. This is unacceptable where the output is displayed in X, Y, Z coordinates or any other form ordered in time, frequency, and intensity. In such a display, where X is time, Y frequency, and Z intensity, the variations caused by SWR would appear as continuous black and white bands. These variations are particularly undesirable as they resemble so closely in character the information produced by Solar emissions.

The directional properties of a log-periodic, while advantageous in some applications, require some accommodations which are not justifiably productive in the particular operation considered here. Because of the directive characteristic of the log periodic, mechanical tracking for a Solar patrol would be required. In the dekameter band this necessitates a device of considerable size and strength. It is also relatively vulnerable to damage or destruction from extremes of weather. The tracking feature also dictates that the antenna be mounted several wavelengths above ground, 60 to 100 ft. This immediately prevents the use of shielding to decrease line-of-sight interference; a critical requirement for sites within 50 miles or so from populated areas.

It would seem for a system which will monitor the relatively strong emissions from the sun $> 10 \times 10^{-22}$ W/m^2/Hz and where position information is one of the desired products, an array of 2 or more fixed broad band dipoles, properly situated to achieve resolving power, would be adequate to serve as an antenna system. The beam of the antenna should be broad enough in one plane to receive, with uniform efficiency, emissions from the sun during its course from sunrise to sunset.

Summing up these considerations, it was decided the characteristics of an antenna for this application should:

(1) Be a simple physical structure,

(2) Have minimum effects from ground reflections,

(3) Have minimum effects from RFI, particularly line-of-sight,

(4) Have a radiation pattern roughly the shape of a half dougnut for continuous observation of the sun without mechanical tracking,

(5) Have wide band frequency response, flat to 0.5 dB,

(6) Have a SWR less than 1.5:1.

Present knowledge indicates that, in antenna design, a cone is the simplest and most efficient shape which will achieve broad band frequency response. Two cones or a combination of a disc and cone can be used as the quarter-wave elements to form a dipole (see Figure 11). They are most commonly used in a vertical mount to produce uniform horizontal radiation. These considerations led to the design and construction of a model antenna scaled down to manageable size for operation

in the 200 to 600 MHz band. This is shown in Figure 12. It consists of two half cones mounted as the elements of a horizontally polarized dipole. The effect of a half cone with the open side facing ground could only be roughly estimated by theory. It was determined experimentally that when the antenna in this configuration was placed above ground a distance equal to 1/8 wavelength of the lowest frequency of the design bandwidth (f_1) the ground effects were least and the radiation pattern was close to the desired half doughnut shape.

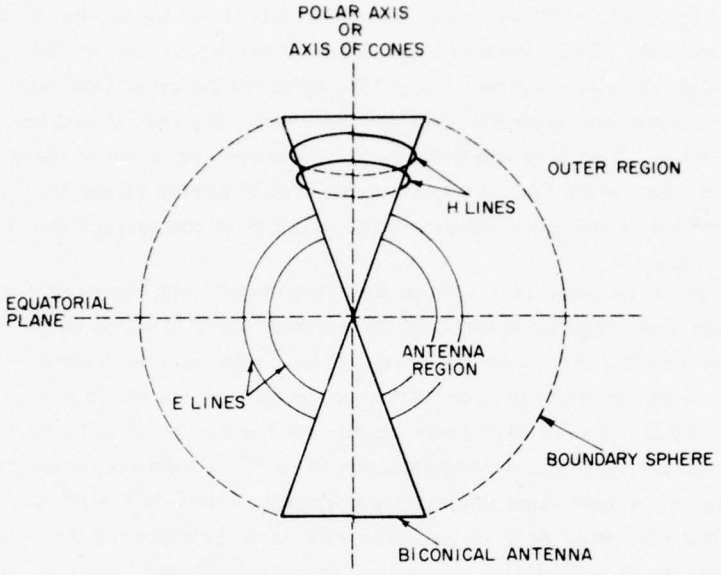

Figure 11. Biconical Antenna, Theory

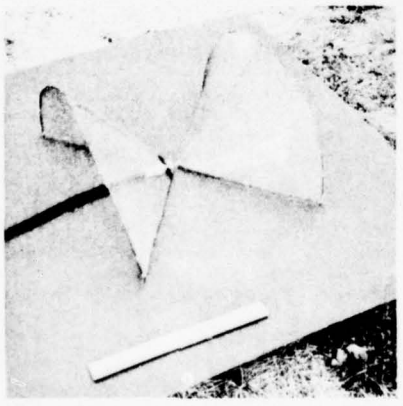

Figure 12. Half Bicone Antenna UHF Band

The VSWR of this configuration scaled up to the 20 to 80 MHz band was measured. The results are shown in Figure 13 compared with a log periodic antenna and calibrated load. A prototype of the final version of the semi-bicone antenna is shown in Figure 14. The relatively small spacing between the antenna and ground permits installation where one can take advantage of terrain or other shielding to reduce effects of line-of-sight interference. The beam pattern is approximately as shown in Figure 15. Precise pattern measurements of the scaled up model were not possible because of the distances involved in measuring the far field in the dekameter band. Figure 16 shows one of the satellite records from which the approximate pattern was derived. The two antennas, log period and bicone, were in a fixed position. The satellite bearing and distance are noted at three points on the record. Several such records were necessary to arrive at the approximate pattern. The most significant feature of the records is the smoothness and absence of secondary lobes.

A drawing of the antenna scaled in wavelengths of f_1 is shown in Figure 17. Both the beam shape and impedance of the antenna are a function of the half-cone angle. Their relationship is shown in Figure 18.[6] It would be desirable to produce a narrow beam in the plane perpendicular to the axis of the cones and to have an impedance of 50 Ω. These objectives would require a relatively large half-cone angle and considering that the total size and area of the antenna would increase exponentially as the half-cone angle, it was decided that a 50° half-cone angle would permit a structure of practical size with an impedance of 90 Ω which could be easily matched to a 50-Ω transmission line. An additional feature, which could be predicted only roughly in theory, is the relatively sharp nulls in the direction, on either side, projected from the axis of the cones. If site location permits, the placing of these nulls toward locations of strong line-of-sight interference will substantially reduce its effect.

6. Kraus, J. D. (1950) Antennas, McGraw Hill, p. 222.

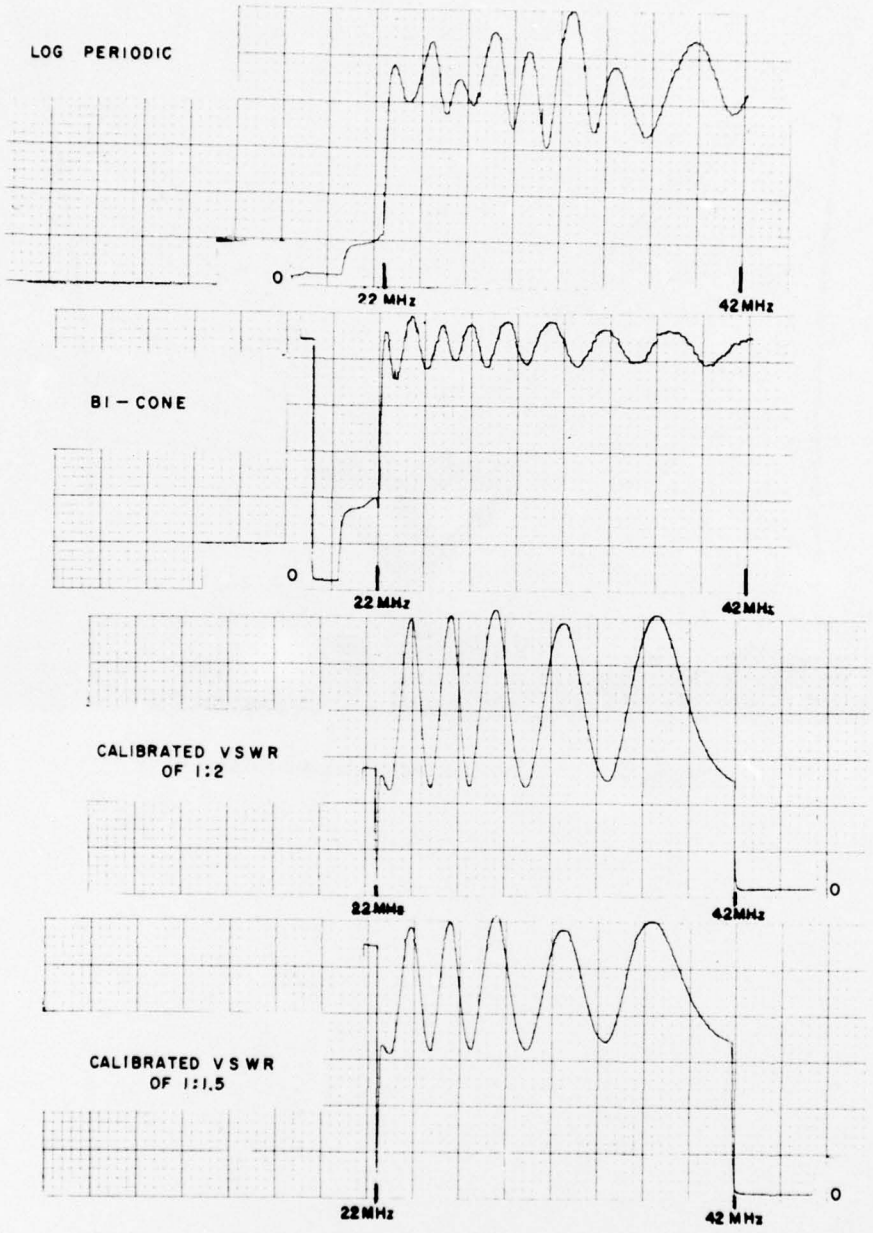

Figure 13. Impedance Variations vs Frequency from which VSWR Measurements of the Bicone Antenna Were Derived

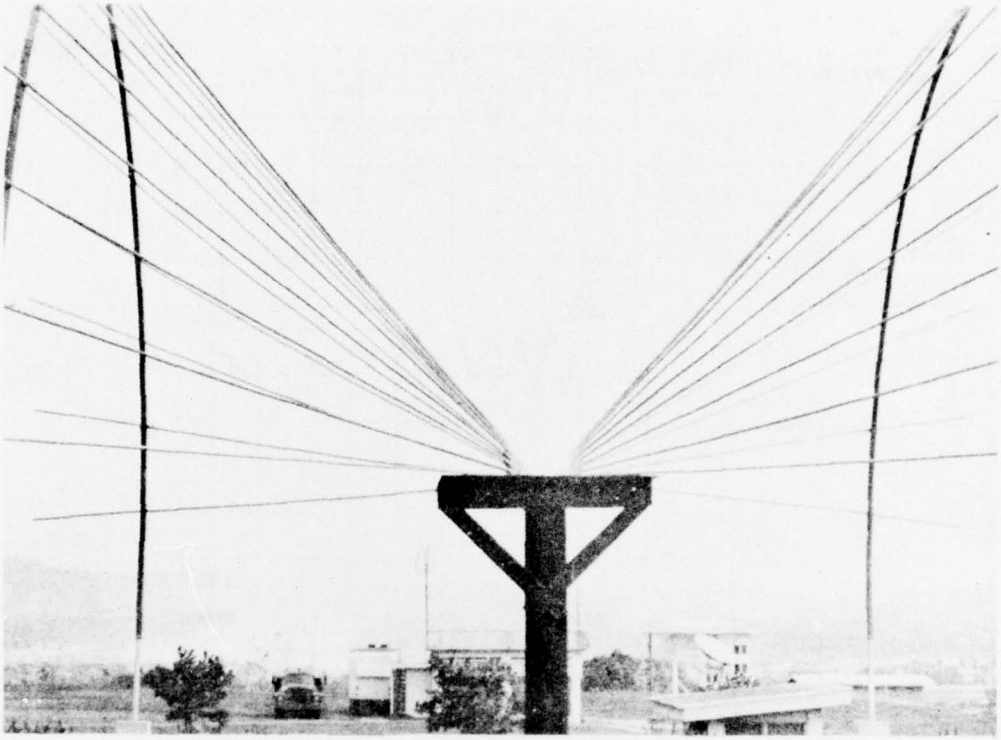

Figure 14. Half Bicone (Semi-Bicone) Antenna

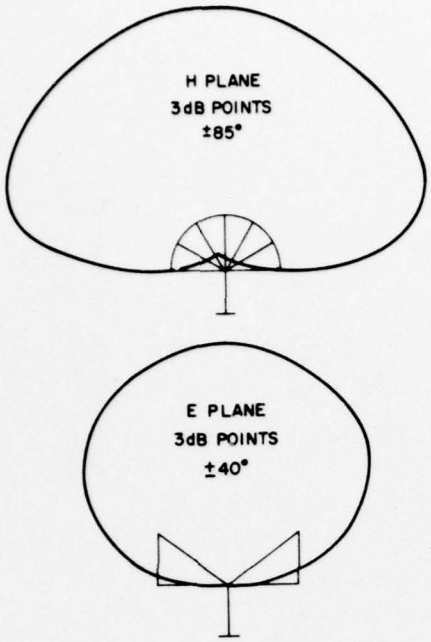

Figure 15. Approximate Beam Pattern of Semi-Bicone Antenna

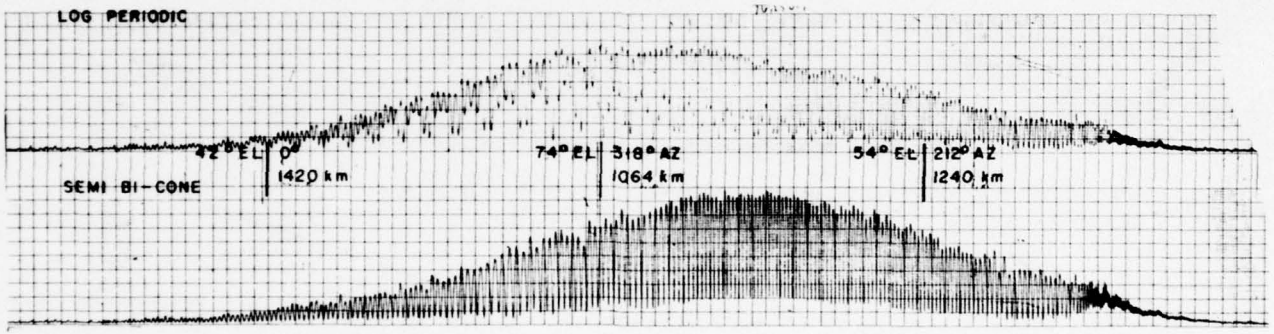

Figure 16. 20 MHz Satellite Signal as Received by Semi-Bicone Antenna and Log-Periodic Antenna

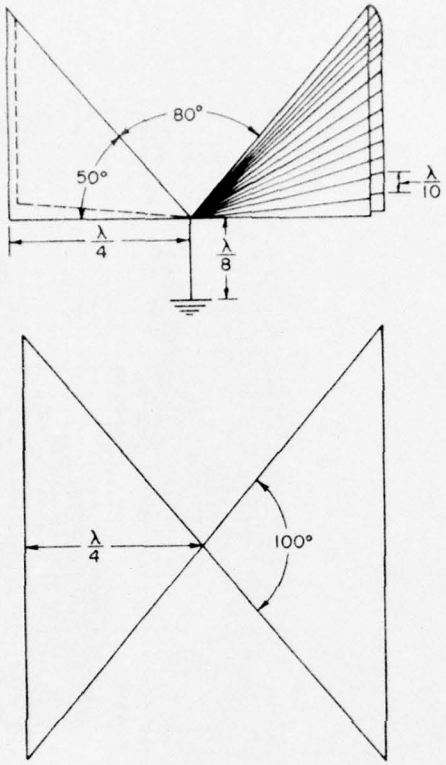

Figure 17. Semi-Bicone Antenna Scaled in Wavelengths of Lowest Frequency in Design Bandwidth

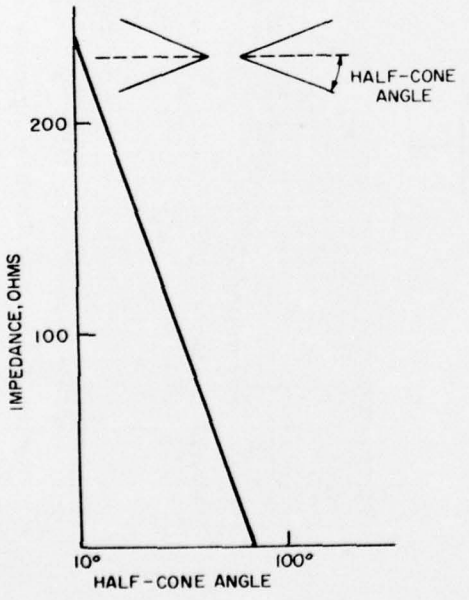

Figure 18. Impedance of Bicone Antenna

4.2 Receiver

In the last decade or so, demand for wide band, sensitive, precise measurements of the radio spectrum has become sufficiently widespread to encourage the manufacture and sale of well engineered, relatively low cost, spectrum analyzers which include all of the requirements of a precision sweep frequency receiver; accurate tuning, linear frequency sweep, flat response, and sensitivities to -130 dBm. These devices compare favorably, indeed surpass, the specialized systems developed at high cost in the recent past.

The particular device used as a receiver in the Sagamore Hill system is a Hewlett Packard Spectrum Analyzer Model 8552/3 (see Figure 19). It is broadly similar to 10 or 15 others on the market. It has been used satisfactorily in another application at Sagamore Hill.[7] The general specifications required and found in this device are:

Frequency range	1 KHz to 110 MHz (selectable in increments, of 1, 2, 5),
Frequency resolution	10 Hz to 300 KHz,
IF bandwidth shape	60 dB/3 dB ratio - 20:1,
Linearity of sweep	better than 1 percent (verified at Sagamore Hill),
Sweep rate	10 msec to 100 sec, selectable,
Flatness of response	log = 0.5 dB; linear = 5.8 percent,
Sensitivity	to -140 dBm,
Dynamic range	70 dB

The HP system also contains a calibration and test accessory, Hewlett Packard Tracking Generator Model No. 8443B, which generates an RF signal synchronized with the receiver sweep so that its frequency is always the same as that to which the receiver is tuned. This calibration device will also serve as a reference in an automatic source position resolving circuit envisioned for the future. At Sagamore Hill the output of the tracking generator is coupled to the transmission lines at the base of each antenna. This arrangement provides a simple and efficient means of operational periodic calibration of the system sensitivity, gain, and phase resolution.

7. Gaunt, D.N. (1975) AFCRL Tech Rpt. 75-0262.

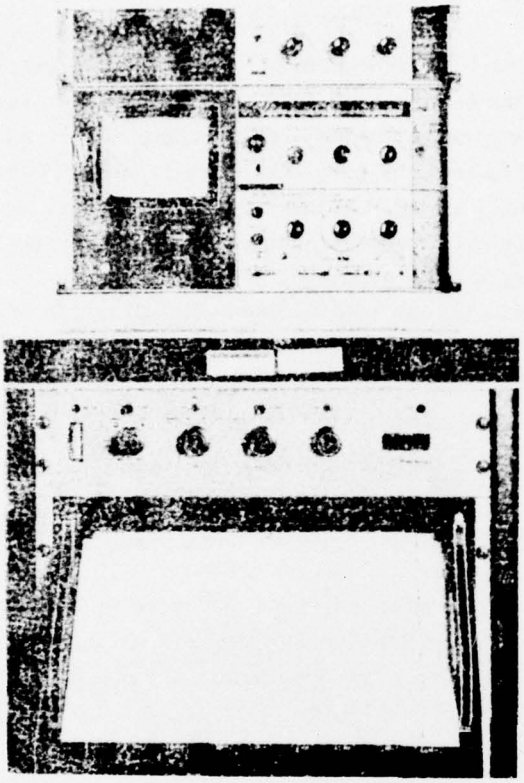

Figure 19. Photo of SFIR Receiver and Recording System

4.3 Detector

Immediately following the receiver is the phase detector, floating clipper, and switch reference generator circuit as shown in Figure 20. The floating clipper acts to reduce the effects of interference by clipping strong manmade transmissions that rise above the background noise (composite of receiver, sun, sky). Figure 21 illustrates the clipping action. The level of clip automatically rises and falls in proportion to changes in the background noise, maintaining a level of clip just above it. This achieves effective elimination of interference and at the same time permits reception of the large range of solar signals (60 dB). At each point in the sweep where clipping takes place, the signal from the receiver is blanked out by insertion of a bias signal equal to the mean value of the background, thus introducing effectively a zero signal to the ac-coupled band pass filter (2500 MHz switching signal) in the next stage. This reduces the amount of noise in the information band introduced by the clipping action. The integration time for averaging background

noise is determined by an RC filter with a time constant of approximately 10 sec or 10 sweeps.

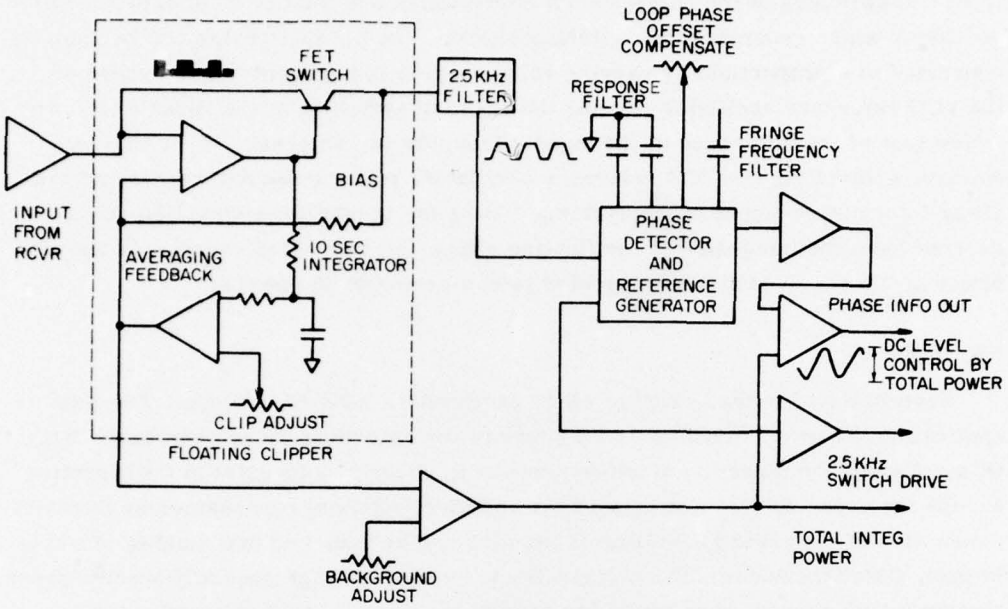

Figure 20. Floating Clipper and Phase Detector, Logic Diagram

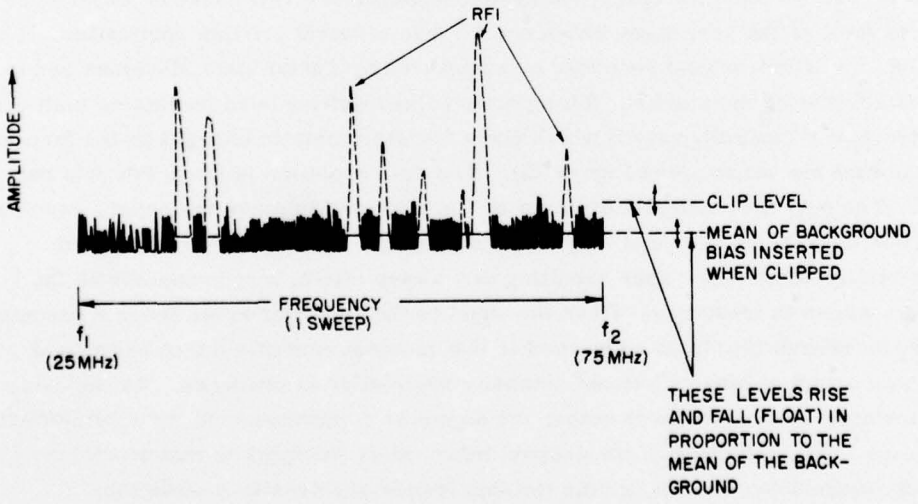

Figure 21. Floating Clipper Action

The phase detection process is achieved by an integrated circuit, phase-locked loop. At the input of this phase-locked loop, the phase of the modulation caused by front end switching of the Dicke Switch is compared with that of a voltage-controlled-oscillator which generates the switching signal. The product of this comparison is converted to a proportionally varying voltage which in turn controls the phase of the VCO reference oscillator causing the phase of switching at the Dicke Switch to follow that of the difference of the signals from the two antennas. This varying voltage, controlling the VCO reference oscillator, is recorded and represents the phase information output of the system. There is, in addition to this, an output derived from the integrator of the floating clipper circuit which represents the total power of the received signal integrated over a period of 10 sweeps.

4.4 Display

Several devices are available which can produce XYZ recordings. For this application the two dimensions in the plane of the recording paper represent: time (X axis) along the direction of paper movement, frequency (Y axis) in the direction across the paper 90° from the time axis, intensity (Z axis) represented by intensity modulation of the record. Writing or printing can be achieved in a number of ways; impact, (like typewriter), varying electrical current through specially treated paper, photographic process, heat applied to special paper, ink, or a relatively new process whereby electrostatic charges are placed with sharp definition on specially treated paper and then exposed to a solution in which carbon particles are suspended. These particles adhere to and make visible,the charged areas. This latter process was selected for use in the system at Sagamore Hill based on experience with several of the processes which proved less efficient for this application. The device is an electrostatic recorder manufactured by Varian Data Machines and is one of several on the market. These have a fixed writing head containing multiple electronically controlled stylii which place the electrostatic charges in the form of dots across the paper, (see Figure 22). The dot resolution is 80 to 100 dots per inch. The only mechanical movement is that required to move the paper, resulting in minimum maintenance and long time reliability. The stylii are addressed sequentially across the paper resulting in a sweep effect, synchronous with the system sweep in frequency. When the input to the recorder rises above a predetermined threshold, the stylus addressed at that moment causes a dot to be printed. In this way a sort of binary "off-on" intensity modulation is produced. As the data, particularly at low levels is noise, the signal as it increases causes a proportionate increase in the definition of the desired information (fringes) so that an effective density modulation results, giving the appearance of intensity modulation.

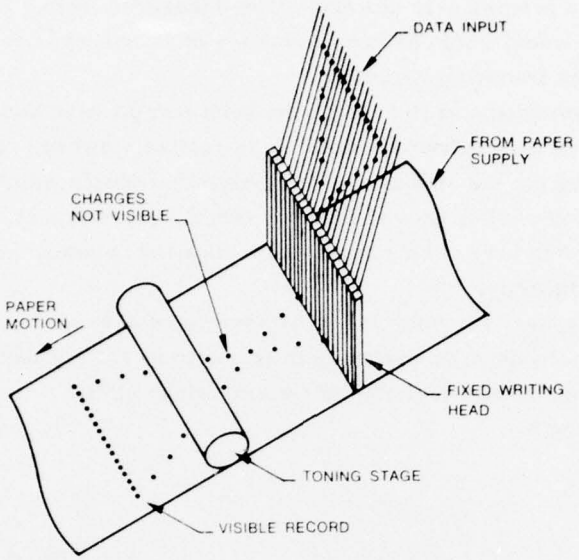

Figure 22. Electrostatic Recorder

In order to provide the XYZ recorder with a fourth input to supplement the Z intensity axis, a circuit combines the phase information and average total power information so that the phase information (sinusoidal ac) is shifted up or down in the dc domain relative to the print threshold on the recorder. This produces fringe width modulation proportional to amplitude. This function is schematically illustrated in Figure 23. This feature, fringe width modulation, provides an important and useful function in spectral display, the ability to distinguish time-intensity profiles of simultaneous high amplitude emissions such as a Type II superimposed on a strong Type IV background. In systems of limited dynamic range such events are obscured. Figure 24 shows a fringe width modulation test record made by using the tracking generator output coupled to the transmission line at the base of the two antennas and stepping the output through a range of 60 dB that is the equivalent of the range expected from the solar emissions in the meter and dekameter band.

4.5 Automatic Position Resolving Provision

In a swept frequency interferometer system, such as that described here, the elements of the output data which contain precise source position information are the location and separation of the fringes in the frequency domain. The most critical task, in automatically determining the fringe positions, is establishing precisely the frequency scale against which the fringe position is measured. There are several ways of achieving this. Two of the most obvious are:

(1) Assuming a precise rate of sweep; time measured from a reference, such as the start of the sweep, could be representative of frequency,

(2) Measure the frequency directly.

The first method seems at first to be the least complicated and most efficient. However, in practice it is extremely difficult to realize a sweep precision (linear with time) necessary for the kind of position resolution sought which is in the order of a few minutes of arc. The second method, direct measurement of frequency, is the approach suggested here. This technique makes the measurement independent of sweep rate and linearity.

The inputs necessary for this type of measurement are:

(1) Frequency observed at any moment of sweep to 0.1 percent,

(2) Sine function of time (relation of time to fringe shift),

(3) Signal strength.

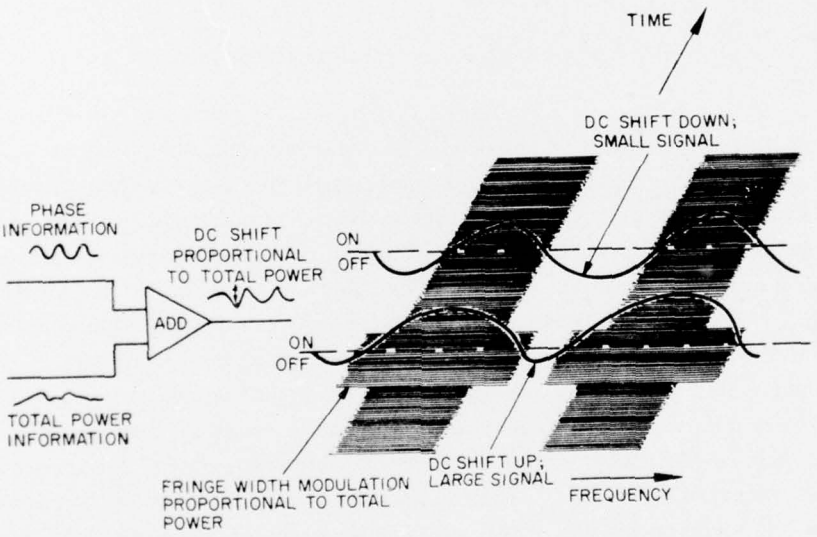

Figure 23. Fringe Width Modulation

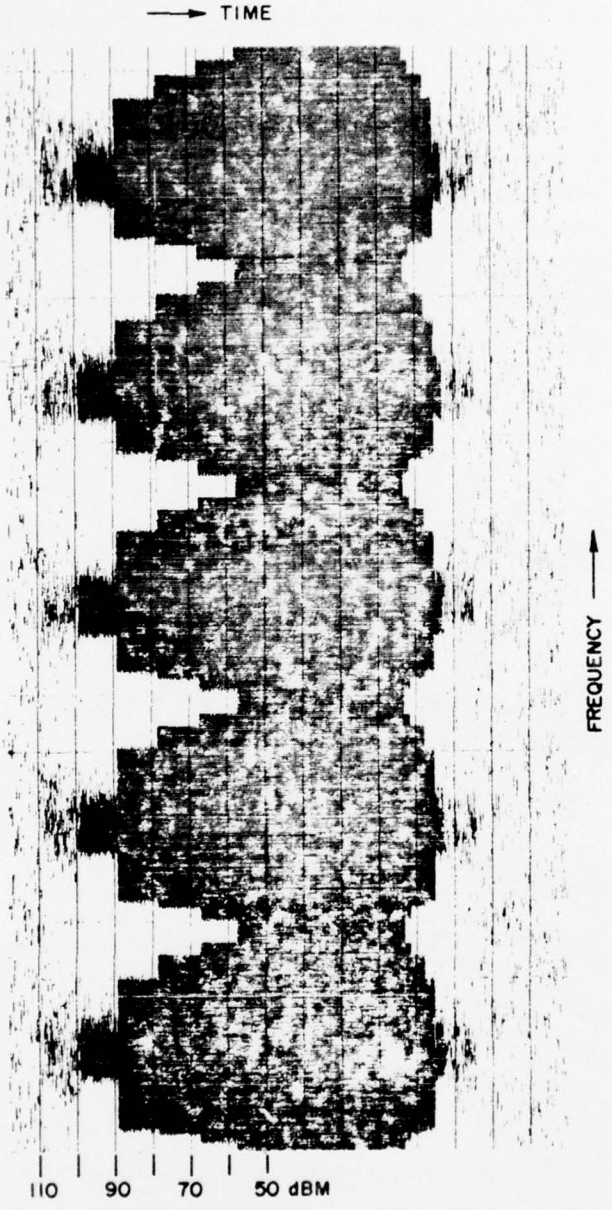

Figure 24. Test of Fringe Width Modulation

Figure 25 shows the proposed system. The first factor is derived from the tracking generator. The second factor, sine function of time, would be generated by digital or analog control of an oscillator to cause its frequency to shift at a sinusoidal rate with time. These two, the frequency proportional to that observed and a frequency proportional to the sine function of time are mixed forming a basic reference from which a gate time is derived. This gate is applied to the system output forming, in a sense, an inertialess filter passing the data with an efficiency proportional to how close the source is from the center of the sun and noting automatically which direction it is displaced. The product of this circuit is fed back to the gate time generator to steer it for maximum response. The amount of steering is the final measure of the source displacement from the center of the sun and is the output of the system. Figure 26 is a logic representation of the operation of the gating technique.

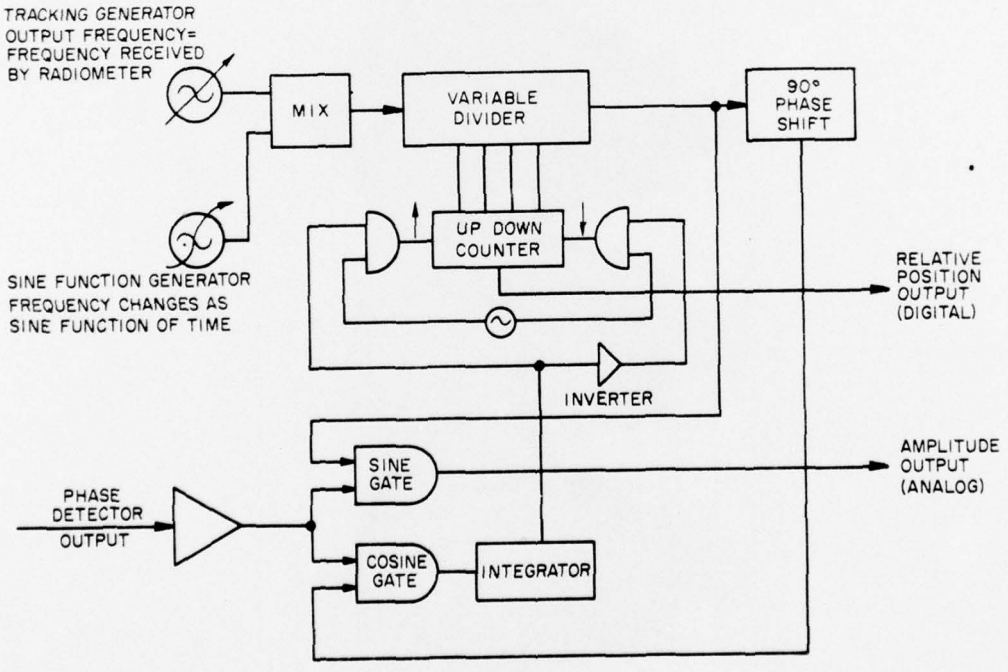

Figure 25. Position Resolving System, Logic

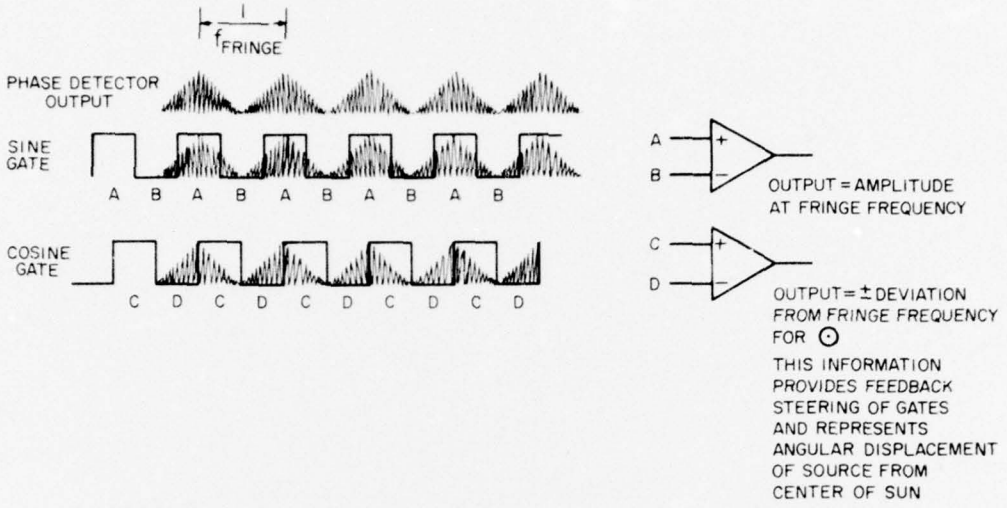

Figure 26. Operation of Sine and Cosine Gates

References

1. Hey, J.S. (1946) Nature 157:47.
2. Boischot, A. and Denisse, K.V. (1957) Compt. Rend., 245:2199.
3. Wild, J.P. and Sheridan, K.V. (1958) Proc. IRE, 46(No. 1):160.
4. Steinberg, J.L. and Lequeux, J. (1963) Radio Astronomy, McGraw Hill, p. 26.
5. Kraus, J.D. (1966) Radio Astronomy, McGraw Hill, p. 258.
6. Kraus, J.D. (1950) Antennas, McGraw Hill, p. 222.
7. Gaunt, D.N. (1975) AFCRL Tech Rpt. 75-0262.